Carbon 132 (2018) 59–64

Contents lists available at ScienceDirect

Carbon

journal homepage: www.elsevier.com/locate/carbon

The mechanics of energy dissipation in a three-dimensional graphene foam with macroporous architecture

Pranjal Nautiyal, Benjamin Boesl, Arvind Agarwal*

Nanomechanics and Nanotribiology Laboratory, Department of Mechanical and Materials Engineerings, Florida International University, Miami, FL 33174, USA

ARTICLE INFO

Article history:
Received 5 December 2017
Received in revised form
7 January 2018
Accepted 4 February 2018
Available online 9 February 2018

Keywords:
Graphene foam
Energy dissipation
Mechanics
Nanoindentation

ABSTRACT

The three-dimensional porous architecture of graphene foam combines extraordinary mechanical properties of graphene with a unique structural organization to produce a strong, lightweight material. In this study, mechanisms for energy dissipation in graphene foam are investigated by localized nano-scale dynamic mechanical testing. Mechanical response of the material subjected to cyclic loading-unloading is captured as loss tangent ($\tan\delta$), characterizing the energy dissipation. Indentation tips with different geometries and dimensions (from 100 nm to 100 μm) are employed, which translate into variable stress-states with mechanical stresses ranging from a few kilo-Pascals to a few giga-Pascals. Formation of dynamic ripples, flattening of intrinsic corrugations, kink band formation, inter-layer van der Waals spring-like action, and membrane vibration are proposed as the key energy dissipation mechanisms in graphene foam. The relative contribution of these mechanisms towards energy dissipation is compared and quantified, with $\tan\delta$ values varying from about 0.1 to 0.45. The energy dissipation behavior of the material is found to be highly stable, as the loss tangent values are retained for as high as 50,000 cycles. The fundamental understanding of intrinsic mechanics will enable engineering of impact-tolerable foam structure with desirable and predictable mechanical performance.

1. Introduction

Two-dimensional graphene, with sp^2 hybrid bonded C atoms, has the remarkable in-plane mechanical strength (130 GPa) and stiffness (1 TPa) [1]. Its impressive mechanical properties have inspired the development of free-standing three-dimensional macro-architecture of graphene, to be able to harness its extraordinary electrical and thermal transport properties for wide-ranging potential applications such as sensing [2,3], stretchable electronics [4], energy conversion and storage [5], radiation shielding [6], tissue engineering [7], and as sorbent materials [8]. One of the highly desirable attributes of 2D graphene is its very high surface area, facilitating the superior transfer of stress, electrons, and phonons [9]. Aggregation of 2D graphene to form a porous foam results in a 3D architecture, while at the same time preserving the intrinsic 2D structure and high surface area [10]. Graphene foam has interesting anatomy, consisting of hollow branches and node junctions formed by multiple layers of graphene. This interconnected network provides seamless pathways for stress transfer upon mechanical loading. A combination of intrinsic mechanical properties of graphene and the effect of the 3D architecture makes their mechanics unique. *In situ* tensile deformation of graphene foam revealed rotation and alignment of branches so that the in-plane properties of graphene are exploited for superior load bearing and failure prevention. During compressive loading of graphene foam, bending and elastic compression of branch walls takes place [11]. Mesoscopic modeling of tensile deformation revealed a transition of stress-state from non-concentrated to highly-concentrated with the increase in mechanical strain. As a result, graphene foam stretches while retaining its structural integrity for low strain values but exhibits opening tearing at higher strains [12]. Wang and co-workers reported microstructure rearrangement, such as self-folding and rotation of graphene flakes constituting the foam during deformation. The foam has near-zero Poisson's ratio, which is attributed to microstructure compaction, as the flakes fill the space during deformation and enhance the load bearing capability [13]. 3D cellular graphene monolith is reported to be highly superelastic, capable of recovering from more than 80% compression [14]. These 3D graphene structures can withstand loads greater than 50,000

* Corresponding author.
E-mail address: agarwala@fiu.edu (A. Agarwal).

https://doi.org/10.1016/j.carbon.2018.02.028
0008-6223/

times of their weight without collapsing!

The porosity of these foams approach 99%, and they are extremely light (with densities less than 5 mg/cm^3). The extraordinary specific tensile strength (σ_T/ρ) and Young's modulus (E/ρ) of 3D graphene foams make them highly suited for protection against impact and absorption of mechanical shock [15]. This is evidenced by high energy loss coefficients (in the range of 67–87%) obtained during cyclic compression [14]. These values surpass loss coefficients for conventional foams based on carbon, metals, and polymers. Therefore, graphene foam is an extremely promising material with ***unmatched capability*** for energy dissipation applications. Damping capability of graphene foam has potential applications in aircraft and automobile bodies, precision systems, turbomachinery, sensors, acoustic devices, robotic components, grippers, and nano/micro-electromechanical systems. Our group exploited this property of graphene foam to induce superior damping in polyimide nanocomposite. An improvement in loss tangent as high as 300% was reported due to merely 1.5 wt. % graphene foam addition to the polyimide [16].

It is noteworthy that the energy dissipation in graphene foam would be dependent on its structural organization. Three-dimensional graphene frameworks have been synthesized by numerous approaches, such as chemical vapor deposition [10], hydrothermal reduction [17], freeze-drying [18], solution-processing [19], 3D printing [20], powder metallurgy [21], hard-templating [22] and sol-gel reaction [23]. These approaches result in the different arrangement of graphene flakes, the nature of bonding/interactions between them, the porosity of the foam and the pore size. To be able to control the processing for obtaining graphene foam with desirable and predictable energy loss characteristics, it is important to gain insight into the fundamental mechanics of energy dissipation in the material. While cyclic compression studies reported in the literature provide an understanding of overall energy dissipation by a bulk structure [14], investigations of localized dynamic mechanical response will provide an insight into the constitutive mechanisms that produce such excellent impact absorption capability in graphene foam.

In this study, dynamic mechanical properties of 3D graphene foam are investigated by nanoindentation technique. Nanoindentation probes with different geometries and diameters varying from 100 nm to 10 μm are employed to induce a wide range of stresses (from a few kPa to a few GPa) in graphene foam. The tests capture the effect of contact volume, contact geometry, and nature of stresses induced by the tips on the dynamic mechanical response of the material. The objective is to study the evolution of damping mechanisms in different stress-regimes. These dynamic mechanical investigations were conducted for 50,000 cycles to develop an understanding of energy dissipation by graphene foam over a large number of cycles.

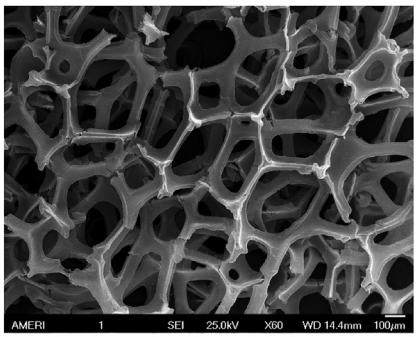

(A)

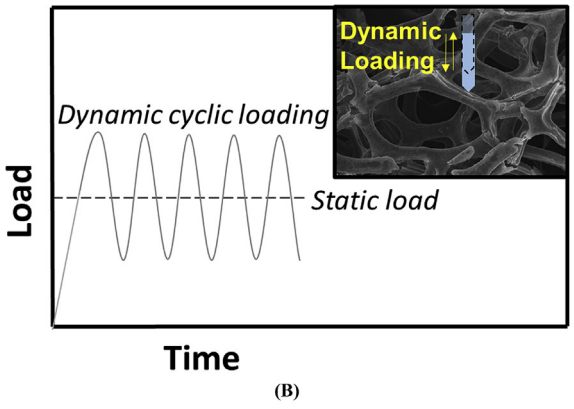

(B)

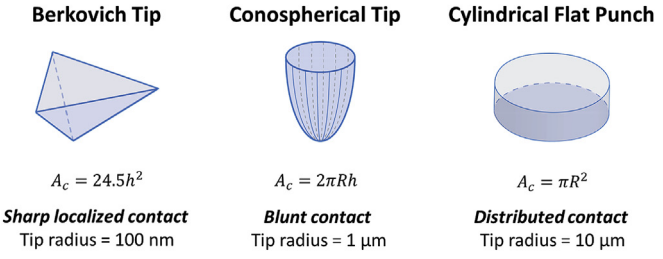

(C)

Fig. 1. **(a)** Scanning electron micrograph of a macroporous three-dimensional graphene architecture, **(b)** a cyclic dynamic loading-unloading profile during nanoindentation (location of indentation is shown in the inset), and **(c)** schematic representation of the geometries of nanoindentation tips used for the dynamic mechanical study. Area functions corresponding to these tips are mentioned in the figure. (A colour version of this figure can be viewed online.)

2. Experimental

The free-standing 3D graphene foam material received from Graphene Supermarket (Calverton, NY, USA) is characterized by a density of 4 mg/cm^3 and pore size of ~580 μm (Fig. 1a). The branches of the graphene foam are hollow, with a diameter of ~50 μm. Damping behavior of graphene foam was investigated using the nanoscale dynamic mechanical analysis (nano-DMA) module of the Hysitron Triboindenter TI-900 (Minneapolis, USA). In nano-dynamic testing, a static load is applied first by the indenter tip, on top of which a cyclic dynamic load is applied with a certain frequency (Fig. 1b). These dynamic indentation tests were performed on the branches of the graphene foam (schematically shown in the inset of Fig. 1b). In this study, the static and dynamic indentation loads of 5 μN and ±500 nN are used, respectively. Typical environment sources produce vibrations in the range of ~60–200 Hz [24]. The performance of nano-devices and structures can be significantly affected/disturbed by the environmental factors. Therefore, the dynamic mechanical tests were carried out at two constant frequencies towards the upper limit of this range: 150 Hz and 210 Hz, to examine the effectiveness of graphene foam in mitigating environmental vibrations. These tests were performed using three different tip geometries and tip dimensions: a Berkovich tip of 100 nm diameter, a Conospherical tip of 1 μm diameter and a cylindrical flat punch of 10 μm diameter (Fig. 1c). The tests were performed for 50,000 dynamic cycles to examine the long-term damping capability. At least 20 dynamic indentation tests were conducted in different regions of the specimen for each

test condition to validate the repeatability of the experiments. The dynamic mechanical response from the material was recorded and analyzed as loss tangent (tan δ).

3. Results

Application of dynamic mechanical load results in a phase lag (δ) between the applied load and the displacement response due to energy dissipation mechanisms activated in graphene foam during cyclic loading-unloading [25]. Due to this phase lag, modulus of the material can be expressed as a combination of storage and loss moduli: $E^* = E' + iE''$ [26]. The storage modulus (E′) is representative of the material's capability to store potential energy, and loss modulus (E″) is the component of energy dissipated during the loading cycle [27]:

$$E' = \frac{\sigma}{\varepsilon}\cos\delta \tag{1}$$

$$E'' = \frac{\sigma}{\varepsilon}\sin\delta \tag{2}$$

The ratio of loss modulus to storage modulus is loss tangent ($\tan\delta = E''/E'$), which is a measure of damping or energy absorption in a dynamic mechanical loading cycle [28]. The loss tangent values as a function of tip geometries and dynamic loading frequencies are plotted in Fig. 2. Small and sharp pyramidal tip (100 nm) induces superior energy dissipation in graphene foam, as evidenced by the loss tangent values as high as ~0.45. This is indicative of up to 45% of mechanical energy dissipated by the material. As the tip size increases, the loss tangent value drops. The flat cylindrical punch with 10 μm diameter exhibits the lowest loss tangent (~0.05–0.15) and conospherical tip with an intermediate value of tip diameter (1 μm) shows loss tangent values in the range of ~0.15–0.30. The loss tangent increases with increasing loading frequency (Fig. 2). It is important to note that the graphene foam retained its damping characteristics for as high as 50,000 cycles, evidenced by stable loss tangent. This attests the suitability of graphene foam in dynamic applications, especially where fatigue resistance is important. The variation of loss tangent for different tips is due to different dynamic mechanisms activated under variable stress-states. The difference in stresses induced by the tips is as high as six orders of magnitude (from 1.5 kPa to 4.63 GPa), summarized in Table 1. We propose intrinsic, inter-layer and macro-architectural damping mechanisms in graphene foam that make them highly damage-tolerable. While ripple wave formation and propagation, and flattening of intrinsic corrugations are the dynamic deformation mechanisms intrinsic to 2D graphene, kink band formation, and van der Waals spring-like action are activate between different layers of graphene assembly. Also, the hollow graphene foam wall vibration also contributes towards energy dissipation. We have quantified, analyzed and categorized these mechanisms based on the stress regimes that favor their activation in the subsequent discussion in detail.

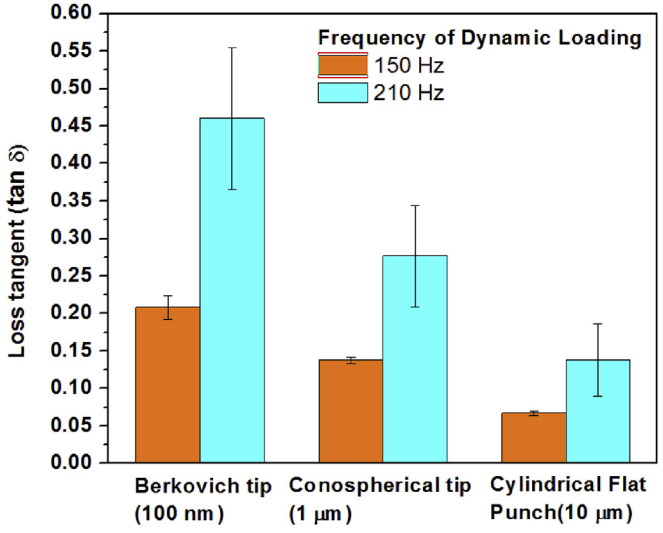

Fig. 2. Loss tangent in nanodynamic mechanical testing for different indenter tips, as a function of dynamic loading frequency. (A colour version of this figure can be viewed online.)

4. Discussion

4.1. Intrinsic 2D energy dissipation mechanisms

During dynamic nanoindentation, the indenter tip exerts repulsive forces on the surface atoms, which is modeled as [29]:

$$F(r) = \begin{cases} -K(r-R)^2, & r < R \\ 0, & r \geq R \end{cases} \tag{3}$$

where K is a force constant, R is the radius of the indenter and r is the distance from the atom to the center of the indenter. This repulsive interaction distorts surface atomic bonds. The distortion of C-C bonds is believed to be responsible for ripple formation in graphene [30]. The formation and propagation of ripples in graphene during dynamic indentation loading leads to absorption of energy [25]. 2D graphene crystal is characterized by the presence of thermodynamically stable edge dislocations in the form of pentagon-heptagon pairs [31,32]. It has been reported that dislocation motion is responsible for stretching, rotation, and breaking of C-C bonds in graphene [33]. Therefore, for the creation of ripples in graphene, the applied indentation stress must exceed the Peierls stress to initiate the dislocation motion, which is defined as the maximum derivative of the misfit energy [34]:

$$\sigma_p = max\left[\frac{1}{b}\frac{dW(u)}{du}\right] = \max\left[-\frac{Kba'}{2\pi^2}\frac{\xi u}{\left(\xi^2+u^2\right)^2}\right] \tag{4}$$

where W(u) is the misfit energy over the slip plane, K is the effective elastic constant, b is the Burgers vector, ξ is the core radius of the dislocation and u is the dislocation translation distance. The theoretical values of Peierls stresses (σ_P) obtained using Eq. (4) exceeds 60 GPa [34]. Table 1 summarizes the penetration depths and stresses for the three tips in the nanoindentation dynamic tests conducted on graphene foam. It can be seen that only stresses associated with Berkovich tip (~4.6 GPa) approach the order of magnitude of the theoretical Peierls stress for graphene. It is noteworthy that the actual Peierls stresses would be lower than the theoretical value due to the presence of chemical impurities and structural defects associated with the processing of graphene foam. Therefore, ripple formation is expected to be an active loss mechanism for dynamic loading induced by Berkovich tip (100 nm) which corresponds to very high localized stress, due to dislocation motion. However, for other tips, the indentation stresses are several orders of magnitude lower than the Peierls stress, and therefore, dynamic ripple formation is highly unlikely.

In addition to the formation and propagation of dynamic ripples due to dynamic loading, it is also noteworthy that graphene comprises of intrinsic corrugations/ripples which are quintessential to stabilize a 2D graphene monolayer [35]. When these intrinsic

Table 1
Depth of penetration, area of contact and localized indentation stresses for Berkovich, Conospherical and Flat punch tips.

Tip geometry	Depth nm	Contact area nm^2	Indentation stress
Berkovich (100 nm)	14.65	5.3×10^3	4.63 **G**Pa
Conospherical (1 μm)	13.2	1.1×10^6	6.1 **M**Pa
Cylindrical flat punch (10 μm)	14.3	3.14×10^8	1.5 **k**Pa

corrugations in graphene are subjected to compressive forces by indentation, flattening of ripples might take place. Vargus and co-workers reported the wavelength of the ripples in graphene to be ~70 nm [36]. Berkovich tip is a sharp tip, with 100 nm diameter. Therefore, indentation by Berkovich would suppress hardly one crest of the ripples. Contrary to this, indentation using a flat punch (10 μm diameter) will compress more than 100 crests of the intrinsic ripples (~diameter of tip/wavelength of ripple). Flattening of ripples leads to absorption of impact energy [25]. This mechanism is likely to be dominant for more substantial interfacial contact and distributed stress condition. For sharp pyramidal tips, flattening will not have any significant contribution towards energy loss as the stress is highly localized.

4.2. Inter-layer energy loss mechanisms

Chemical vapor deposition technique produces a multilayer foam, where the foam walls comprise of 5–10 layers of graphene. The energy dissipation in multilayer materials, such as graphite and Ti_3SiC_2 is reported as stress-strain hysteresis and is ascribed to the formation and annihilation of kink bands [37]. The formation of kink bands is believed to be due to the nucleation and growth of the pairs of dislocation with opposite sign (Fig. 3). The localized stresses required to form a dislocation pair ≈ G/30, where G is the shear modulus. The shear modulus of multi-layer graphene is reported to be ~53 GPa [38]. Therefore, the localized indentation stresses should exceed ~1.8 GPa to form a dislocation pair. From Table 1, only stresses associated with Berkovich tip (100 nm) surpass this stress value. Therefore, the kink formation and annihilation during dynamic loading is a likely mechanism for energy dissipation for sharp pyramidal tips, which represent high-stress conditions.

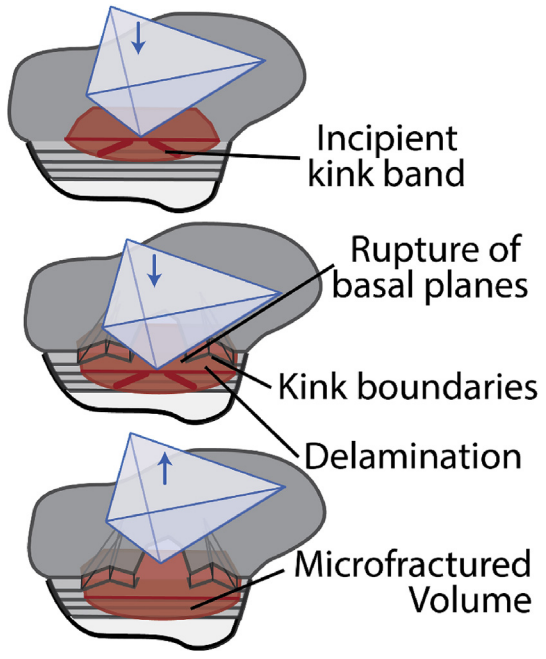

Fig. 3. Schematic representation of energy dissipation in multilayer graphene foam branch walls due to kink band formation. (A colour version of this figure can be viewed online.)

Due to the very high surface area of graphene, there are strong van der Waals interactions between the layers constituting the walls of the foam [25]:

$$P_{VDW} = \frac{A}{6\pi H^3} \tag{5}$$

where P_{VDW} is the van der Waals force per unit area, A is Hamaker's coefficient, and H is the separation between the graphene layers. Therefore, compression due to indentation results in a drop in interlayer distance, H. This inter-layer compression triggers opposing van der Waals forces. This spring-like reaction due to graphene layer compression leads to absorption of indentation impact energy. However, it is noteworthy that after excessive compression, the van der Waals force P_{VDW} approaches exceptionally high values due to very minimal interlayer separation (based on Eq. (5)). Therefore, the in-plane stretching of C-C bonds becomes more favorable than the interlayer compression. Since in-plane deformation is elastic (involving sp^2 C-C bonds), it won't contribute towards energy dissipation. Therefore, the van der Waals interactions contribute towards energy loss ($\tan\delta$) at relatively lower displacements. Vargas and coworkers determined the in-plane breaking stress of graphene to be around 35 GPa [36]. Berkovich tip-induced stresses on the graphene flakes are very high ~4 GPa (Table 1). Although the stresses are lower than the failure stress of 35 GPa, they are high enough to stretch and deform the flakes. Contrary to this, stresses induced by other tips are orders of magnitude lower: ~1.5 kPa for cylindrical punch and ~6 MPa for the conospherical tip. Therefore, energy dissipation due to out-of-plane inter-layer van der Waals interactions is likely to dominate for the conospherical tip and flat punch, since the associated contact stresses are too low to induce in-plane deformation.

4.3. Stress transfer characteristics due to 3D anatomy

In addition to the intrinsic and inter-layer dynamic loss mechanisms, the unique node-branch anatomy of graphene foam also aids in energy dissipation. Due to its hollow anatomy, the wall of graphene foam branch can be considered to be a membrane subjected to loading [39]. The mechanical behavior of the foam branch can be treated using nonlinear Foppl membrane theory [40]. The cubic polynomial function models the indentation load-displacement relationship for such a system:

$$F(h) = \pi\sigma_o^{2D}h + \frac{q^3}{a^3}E_{2D}h^3 \tag{6}$$

where σ_o^{2D} is the membrane pre-tension, E_{2D} is the two-dimensional Young's modulus, a is the radius of the membrane and q is a function of Poisson's ratio ($q \sim 1.0491 - 0.1462\upsilon - 0.15827\upsilon^2$). Contact/interfacial stiffness is obtained by differentiating this expression with respect to h [41]:

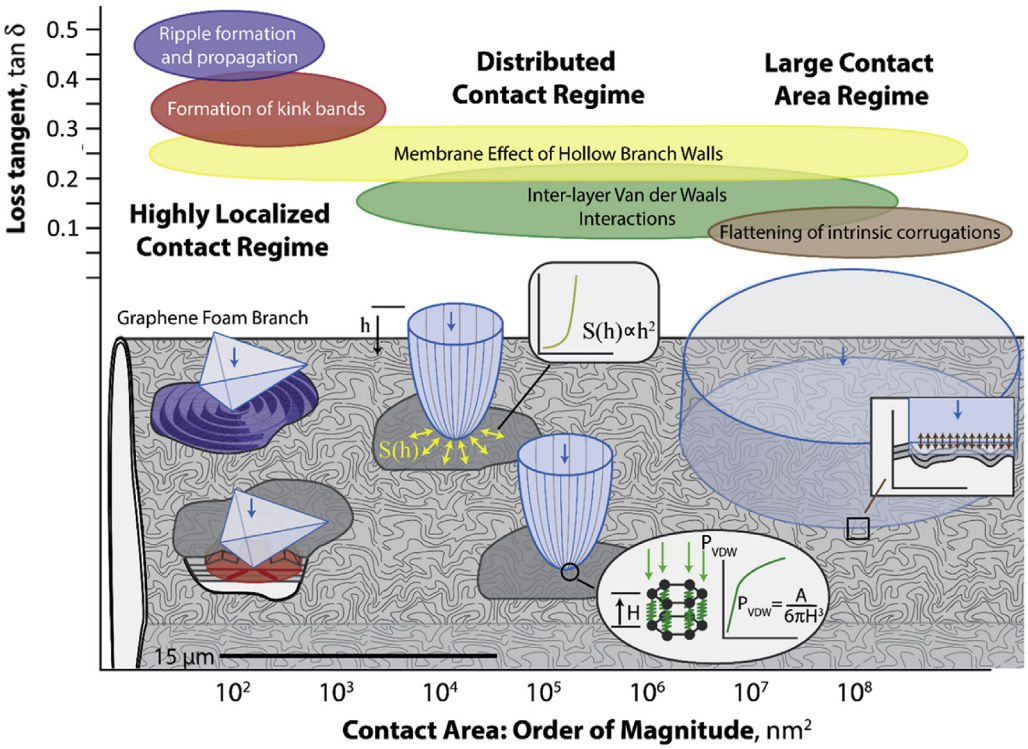

Fig. 4. Schematic representation of energy dissipation mechanisms in a 3D graphene foam that is triggered by variable stress-states. Their relative contribution towards mechanical energy loss is also highlighted. (A colour version of this figure can be viewed online.)

$$S(h) = \frac{dF}{dh} = \pi\sigma_o^{2D} + \frac{3q^3}{a^3}E_{2D}h^2 \quad (7)$$

The contact stiffness for the foam wall varies as a second-degree polynomial with respect to the indentation displacement, h. Therefore, during rapid dynamic loading-unloading of the tip onto the foam wall, the interfacial stiffness would vary significantly (second power of tip displacement). Contact stiffness between the two bodies is intrinsically associated with the covalent bonding in the materials. Therefore, dynamic loading of the hollow foam wall will cause remarkable C-C bond distortion, resulting in the dissipation of vibration energy. This membrane effect for energy dissipation is peculiar to a hollow graphene foam structure, providing it extraordinary shock absorption capability.

The *intrinsic energy dissipation* mechanisms in graphene foam are summarized in Fig. 4, for different stress states simulated by nanoindentation technique.

5. Summary

Energy dissipation behavior of 3D graphene foam was studied by nanoscale dynamic mechanical investigations. Indenter probes with different geometries and diameters were employed to induce a wide range of stresses (varying from a few kPa to a few GPa). The mechanical response was captured as loss tangent (tan δ), which is a measure of energy dissipation by the material. Loss tangent values varying from 0.1 to 0.45 were obtained for different stress regimes and contact volumes during the dynamic testing. A combination of ripple formation, suppression of intrinsic corrugations, kink band formation, interlayer van der Waals interactions and hollow-wall vibration effect result in extraordinary damping capability of graphene foam. By dispersing the force of impact over a wider area, damage localization is avoided in graphene foam, making them impact tolerable. A fundamental understanding of the mechanics of energy dissipation in graphene foam will enable engineering of foam structure to tailor their dynamic mechanical response and induce application-specific damping capability. This study has implications for design and development of 3D graphene-based advanced nanostructures for a wide–range of applications requiring superior structural stability and ability to absorb mechanical impact. A few of these potential applications are scaffolds for tissue engineering, components in robotic devices, sensors, artificial skin, batteries and supercapacitors, and aerospace/automotive structures with vibration damping capability.

Acknowledgements

The authors would like to acknowledge U.S. Department of Defense for W911NF-15-1-0458 grant. PN thanks Florida International University Graduate School for the financial support through Presidential Fellowship. PN and AA also recognize the Engineering Research Centers Program of the National Science Foundation under NSF Cooperative Agreement No. EEC-1647837.

References

[1] C. Lee, X. Wei, J.W. Kysar, J. Hone, Measurement of the elastic properties and intrinsic strength of monolayer graphene, Science 321 (2008) 385–388.
[2] J. Leem, M.C. Wang, P. Kang, S.W. Nam, Mechanically self-assembled, three-dimensional graphene-gold hybrid nanostructures for advanced nanoplasmonic sensors, Nano Lett. 15 (2015) 7684–7690.
[3] L. Embrey, P. Nautiyal, A. Loganathan, A. Idowu, B. Boesl, A. Agarwal, Three-dimensional graphene foam induces multifunctionality in epoxy nanocomposites by simultaneous improvement in mechanical, thermal and electrical properties, ACS Appl. Mater. Interfaces 9 (2017) 39717–39727.
[4] L. Zhang, D. DeArond, N.T. Alvarez, R. Malik, N. Oslin, C. McConnell, et al., Flexible micro-supercapacitor based on graphene with 3D structure, Small 13 (2017), 1603114.
[5] H. Bi, T. Lin, F. Xu, Y. Tang, Z. Liu, F. Huang, New graphene form of nanoporous monolith for excellent energy storage, Nano Lett. 16 (2016) 349–354.

[6] Z. Chen, C. Xu, C. Ma, W. Ren, H.-M. Cheng, Lightweight and flexible graphene foam composites for high-performance electromagnetic interference shielding, Adv. Mater. 25 (2013) 1296–1300.
[7] A. Nieto, R. Dua, C. Zhang, B. Boesl, S. Ramaswamy, A. Agarwal, Three dimensional graphene foam/polymer hybrid as a high strength biocompatible scaffold, Adv. Funct. Mater. 25 (2015) 3916–3924.
[8] H. Bi, X. Xie, K. Yin, Y. Zhou, S. Wan, L. He, et al., Spongy graphene as a highly efficient and recyclable sorbent for oils and organic solvents, Adv. Funct. Mater. 22 (2012) 4421–4425.
[9] C.N.R. Rao, A.K. Sood, K.S. Subrahmanyam, A. Govindaraj, Graphene: the new two-dimensional nanomaterial, Chem. Int. Ed. 48 (2009) 7752–7777.
[10] Z. Chen, W. Ren, L. Gao, B. Liu, S. Pei, H.-M. Cheng, Three-dimensional flexible and conductive interconnected graphene networks grown by chemical vapor deposition, Nat. Mater. 10 (2011) 424–428.
[11] A. Nieto, B. Boesl, A. Agarwal, Multi-scale intrinsic deformation mechanisms of 3D graphene foam, Carbon 85 (2015) 299–308.
[12] D. Pan, C. Wang, T.-C. Wang, Y. Yao, Graphene foam: uniaxial tension behavior and fracture mode based on a mesoscopic model, ACS Nano 11 (2017) 8988–8997.
[13] C. Wang, C. Zhang, S. Chen, The microscopic deformation mechanism of 3D graphene foam materials under uniaxial compression, Carbon 109 (2016) 666–672.
[14] L. Qiu, J.Z. Liu, S.L.Y. Chang, Y. Wu, D. Li, Biomimetic superelastic graphene-based cellular monoliths, Nat. Commun. 3 (2012) 1241.
[15] Z. Qin, G.S. Jung, M.J. Kang, M.J. Buehler, The mechanics and design of a lightweight three-dimensional graphene assembly, Sci Adv. 3 (2017), e1601536.
[16] P. Nautiyal, B. Boesl, A. Agarwal, Harnessing three dimensional anatomy of graphene foam to induce superior damping in hierarchical polyimide nanostructures, Small 13 (2017), 1603473.
[17] Y. Li, J. Chen, L. Huang, C. Li, J.-D. Hong, G. Shi, Highly compressible macroporous graphene monoliths via an improved hydrothermal process, Adv. Mater. 26 (2014) 4789–4793.
[18] C. Hu, J. Xue, L. Dong, Y. Jiang, X. Wang, L. Qu, et al., Scalable preparation of multifunctional fire-retardant ultralight graphene foams, ACS Nano 10 (2016) 1325–1332.
[19] L. Lv, P. Zhang, H. Cheng, Y. Zhao, Z. Zhang, G. Shi, et al., Solution-processed ultraelastic and strong air-bubbled graphene foam, Small 12 (2016) 3229–3234.
[20] J. Sha, Y. Li, R.V. Salvatierra, T. Wang, P. Dong, Y. Ji, et al., Three-dimensional printed graphene foams, ACS Nano 11 (2017) 6860–6867.
[21] J. Sha, C. Gao, S.-K. Lee, Y. Li, N. Zhao, J.M. Tour, Preparation of three-dimensional graphene foams using powder metallurgy templates, ACS Nano 10 (2016) 1411–1416.
[22] X. Huang, K. Qian, J. Yang, J. Zhang, L. Li, C. Yu, et al., Functional nanoporous graphene foams with controlled pore sizes, Adv. Mater. 24 (2012) 4419–4423.
[23] W. Strek, R. Tomala, M. Lukaszewicz, B. Cichy, Y. Gerasymchuk, P. Gluchowski, et al., Laser induced white lighting of graphene foam, Sci. Rep. 7 (2017), 41281.
[24] A. Tiwari, B. Raj, Materials and Failures in MEMS and NEMS, John Wiley & Sons, 2015.
[25] D. Lahiri, S. Das, W. Choi, A. Agarwal, Unfolding the damping behavior of multilayer graphene membrane in the low-frequency regime, ACS Nano 6 (2012) 3992–4000.
[26] K. Balani, A. Agarwal, Damping behavior of carbon nanotube reinforced aluminum oxide coatings by nanomechanical dynamic modulus mapping, J. Appl. Phys. 104 (2008), 063517.
[27] R. Agrawal, A. Nieto, H. Chen, M. Mora, A. Agarwal, Nanoscale damping characteristics of boron nitride nanotubes and carbon nanotubes reinforced polymer composites, ACS Appl. Mater. Interfaces 5 (2013) 12052–12057.
[28] P. Nautiyal, L. Embrey, B. Boesl, A. Agarwal, Multi-scale mechanics and electrical transport in a free-standing 3D architecture of graphene and carbon nanotubes fabricated by pressure assisted welding, Carbon 122 (2017) 298–306.
[29] W. Xia, J. Song, D.D. Hsu, S. Keten, Understanding the interfacial mechanical response of nanoscale polymer thin films via nanoindentation, Macromolecules 49 (2016) 3810–3817.
[30] Y.Z. He, H. Li, P.C. Si, Y.F. Li, H.Q. Yu, X.Q. Zhang, et al., Dynamic ripples in single layer graphene, Appl. Phys. Lett. 98 (2011), 063101.
[31] O.V. Yazyev, S.G. Louie, Topological defects in graphene: dislocations and grain boundaries, Phys. Rev. B 81 (2010), 195420.
[32] A. Carpio, L. Bonilla, Periodized discrete elasticity models for defects in graphene, Phys. Rev. B 78 (2008), 085406.
[33] J.H. Warner, E.R. Margine, M. Mukai, A.W. Robertson, F. Giustino, A.I. Kirkland, Dislocation-driven deformations in graphene, Science 337 (2012) 209–212.
[34] F. Meng, B. Ouyang, J. Song, First principles study of dislocation slips in impurity-doped graphene, J. Phys. Chem. C 119 (2015) 3418–3427.
[35] J.H. Warner, Y. Fan, A.W. Robertson, K. He, E. Yoon, G.D. Lee, Rippling graphene at the nanoscale through dislocation addition, Nano Lett. 13 (2013) 4937–4944.
[36] C.S. Ruiz-Vargas, H.L. Zhuang, P.Y. Huang, A.M. van der Zande, S. Garg, P.L. McEuen, et al., Softened elastic response and unzipping in chemical vapor deposition graphene membranes, Nano Lett. 11 (2011) 2259–2263.
[37] M.W. Barsoum, A. Murugaiah, S.R. Kalidindi, T. Zhen, Y. Gogotsi, Kink bands, nonlinear elasticity, and nanoindentations in graphite, Carbon 42 (2004) 1435–1445.
[38] X. Liu, J.T. Robinson, Z. Wei, P.E. Sheehan, B.H. Houston, E.S. Snow, Low temperature elastic properties of chemically reduced and CVD-grown graphene thin films, Diam. Relat. Mater. 19 (2010) 875–878.
[39] Q. Wang, W. Hong, L. Dong, Graphene “microdrums” on a freestanding perforated thin membrane for high sensitivity MEMS pressure sensors, Nanoscale 8 (2016) 7663–7671.
[40] J. Martinez-Asencio, C.J. Ruestes, E.M. Bringa, M.J. Caturla, Controlled rippling of graphene *via* irradiation and applied strain modify its mechanical properties: a nanoindentation simulation study, Phys. Chem. Chem. Phys. 18 (2016) 13897–13903.
[41] S. Akarapu, T. Sharp, M.O. Robbins, Stiffness of contacts between rough surfaces, Phys. Rev. Lett. 106 (2011), 204301.